Influence of germanium on thermal dewetting and agglomeration of the silicon template layer in thin silicon-on-insulator

2009 J. Phys. D: Appl. Phys. 42 175309

(http://iopscience.iop.org/0022-3727/42/17/175309)

IOP PUBLISHING JOURNAL OF PHYSICS D: APPLIED PHYSICS

J. Phys. D: Appl. Phys. **42** (2009) 175309 (6pp) doi:10.1088/0022-3727/42/17/175309

Influence of germanium on thermal dewetting and agglomeration of the silicon template layer in thin silicon-on-insulator

P P Zhang[1,3], B Yang[1,4], P P Rugheimer[1,5], M M Roberts[1,6], D E Savage[1], Feng Liu[2] and M G Lagally[1,7]

[1] University of Wisconsin, Madison, WI 53706, USA
[2] University of Utah, Salt Lake City, UT 84112, USA

E-mail: lagally@engr.wisc.edu

Received 14 June 2009, in final form 28 July 2009
Published 20 August 2009
Online at stacks.iop.org/JPhysD/42/175309

Abstract

We investigate the influence of heteroepitaxially grown Ge on the thermal dewetting and agglomeration of the Si(0 0 1) template layer in ultrathin silicon-on-insulator (SOI). We show that increasing Ge coverage gradually destroys the long-range ordering of 3D nanocrystals along the ⟨1 3 0⟩ directions and the 3D nanocrystal shape anisotropy that are observed in the dewetting and agglomeration of pure SOI(0 0 1). The results are qualitatively explained by Ge-induced bond weakening and decreased surface energy anisotropy. Ge lowers the dewetting and agglomeration temperature to as low as 700 °C.

(Some figures in this article are in colour only in the electronic version)

1. Introduction

The morphological stability of thin films has been the subject of experimental and theoretical studies for many years (see reviews [1, 2]). In general, if a film of material A on a substrate of material B is thermodynamically unstable, it will roughen or dewet and agglomerate at sufficiently elevated temperatures. The origin of dewetting and thermal agglomeration can be traced to its thermodynamic roots [2], but it is essentially a kinetic process. Dewetting and thermal agglomeration occur in many systems, such as amorphous and polycrystalline thin films sputter deposited or evaporated onto heterogeneous hosts [3–5]. Recently, thermal dewetting and agglomeration of a *single-crystal* thin film, the top Si(0 0 1) layer ('template layer') in silicon-on-insulator (SOI), have been investigated [6–11]. In contrast to amorphous or polycrystalline thin films, the resulting agglomerated silicon nanocrystals self-order in a distinct, thermodynamically controlled pattern that can be exploited as the template for bottom-up nanoassembly and nanofabrication [12].

The thermal dewetting of crystalline Si from, and agglomeration on, its oxide is driven primarily by chemical interactions: whereas SiO_2 is thermodynamically stable on Si, Si is not chemically stable on its oxide. Additionally, strain within the film plays an important role in destabilizing a continuous film. A second class of morphological instability can occur for a heteroepitaxial film on a crystalline substrate, in which misfit strain becomes part of the free-energy balance that determines stability. In such cases misfit strain can induce surface roughening [1]. For instance, controlled annealing of a thin Ge or SiGe film heteroepitaxially grown on a Si substrate causes the film to roughen [13].

In this paper, we report investigations of the thermal stability of ultrathin Ge/SOI(0 0 1). When we grow Ge epitaxially on ultrathin SOI, we combine chemical and strain destabilizing factors into one system. We show that increasing Ge coverage gradually destroys the long-range ordering of 3D nanocrystals along the ⟨1 3 0⟩ directions and the 3D nanocrystal shape anisotropy that are observed in the dewetting of pure SOI(0 0 1). The degree of dewetting and agglomeration at a fixed temperature increases with increasing Ge coverage,

[3] Current address: Physics and Astronomy Department, Michigan State University, East Lansing, MI 48824, USA.
[4] Current address: AMD/IBM Alliance, Yorktown Heights, NY 10598, USA.
[5] Current address: Department of Physics, Montana State University, Bozeman, MT 59717, USA.
[6] Current address: Center for Nano Science and Technology, University of Notre Dame, Notre Dame, IN 46556, USA.
[7] Author to whom any correspondence should be addressed.

suggesting that the higher the Ge concentration, the lower the initiation temperature for dewetting. The results are qualitatively explained by Ge-induced bond weakening and decreased surface energy anisotropy.

Beyond its scientific interest, the topic is also relevant in technology. Ge or SiGe thin films have been incorporated into SOI substrates for applications on SiGe-channel ultrathin SOI pMOSFETs and MODFETs [14, 15]. SiGe-on-insulator (SGOI) is itself a promising substrate, as it combines the advantages of SiGe technology with the advantages of SOI technology [16]. These thin films need to be kept intact during thermal processes in device fabrication. Because thermal dewetting puts an upper limit on the allowable device processing temperature, our studies have potentially a direct impact on the microelectronics industry.

2. Experimental details

The experiments are performed with bonded etch-back SOI(0 0 1) from SOITEC, which comprises a Si handling substrate, a 200 nm buried SiO_2 (BOX) layer and a Si(0 0 1) top (template) layer. The bond in such SOI samples occurs in the centre of the BOX layer, so that the top thin-Si/oxide interface is as perfect as any in which a thermal oxide is grown on Si. We thin the Si layer to 9 nm by repeated dry thermal oxidation followed by wet chemical etching to remove the oxide, and then chemically clean the surface using the triple IMEC procedure [17], ending up with a HF dip to maintain a hydrogen terminated surface. With molecular beam epitaxy (MBE) we deposit from 0 to 6 ML of Ge on the 9 nm thick Si(0 0 1) layer at 510 °C using a variable-position shutter in front of the sample, which allows us to increase the Ge coverage on the sample in discrete steps. The sample is then heated by direct current at 850 °C for 20 s, which causes the Si template layer, covered with increasing amounts of Ge in steps, to dewet and agglomerate into 3D nanocrystals. The dewetting is monitored *in situ* by low-energy electron diffraction (LEED). After agglomeration, the samples are removed from the growth chamber and characterized *ex situ* using scanning electron microscopy (SEM), atomic force microscopy (AFM), and scanning Auger electron spectroscopy (AES). With these techniques we can determine both the local morphology and the local composition as a function of the nominal Ge thickness on the 9 nm Si(0 0 1) layer on the oxide.

3. Results and discussion

For zero Ge coverage, we confirm the same dewetting and agglomeration behaviour in thin SOI as was obtained earlier for clean Si in SOI(0 0 1) [6–10]. Three major differences occur with the addition of Ge. The first is that, at the same annealing temperature and time, more of the template layer dewets as the Ge coverage increases, indicated by the white regions in figure 1, which shows SEM images of the thermal agglomeration of the 9nm Si(0 0 1) layer of SOI for nominal Ge coverages ranging from 0 to 4 ML.

The second major observation differentiating dewetting and agglomeration of the thin crystalline Si(0 0 1) layer of

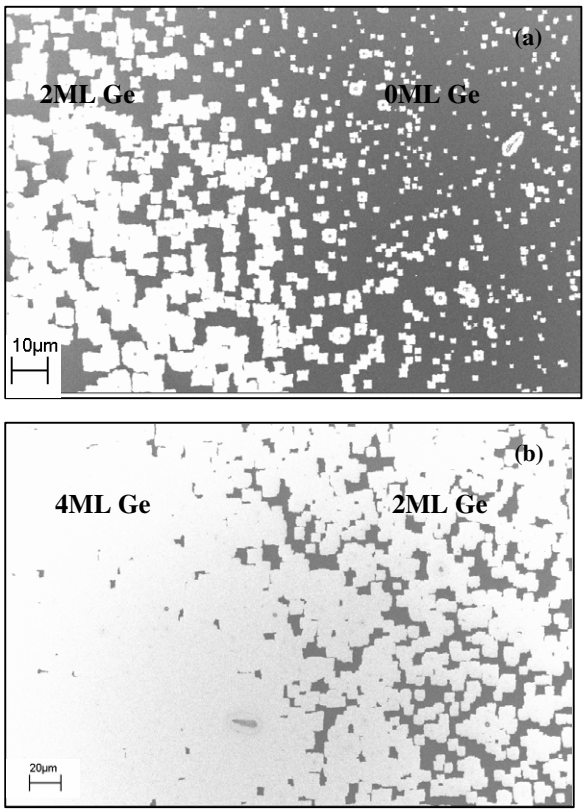

Figure 1. Thermal dewetting and agglomeration of a 9 nm layer of Si(0 0 1) in SOI at 850 °C for 20 s, with different amounts of Ge deposited with MBE at 510 °C. (*a*) SEM image of nominal 0 ML and 2 ML Ge coverage regions. (*b*) SEM image of nominal 2 ML and 4 ML Ge coverage regions. White areas are oxide on which 3D agglomeration islands have formed. When the dewetting is limited, the white agglomeration regions appear as individual squares. When there is greater dewetting, the white agglomeration regions merge. At the same agglomeration temperature, the higher the Ge coverage, the more the Si template layer dewets and forms 3D islands.

SOI in the presence of Ge from that of clean SOI(0 0 1) is the significant loss of long-range order in the agglomerated 3D nanocrystals that form. The higher the Ge coverage is, the lower is the order of the agglomerated nanocrystals. In figure 2, we compare the agglomeration patterns found for SOI(0 0 1) covered by 2 ML of Ge (figures 2(*b*) and (*c*)) and by 6 ML of Ge (figures 2(*d*) and (*e*)) with that found for the clean Si(0 0 1) layer of SOI (figure 2(*a*)). For zero Ge coverage, the agglomerated islands self-align almost uniformly along the ⟨1 3 0⟩ directions [9]. At the lower Ge coverage, we still observe the square, overall anisotropic agglomeration patterns characteristic of the clean-Si dewetting. Near the boundary of the squares, the long-range ordering of the nanocrystals along the ⟨1 3 0⟩ directions remains, the same as in pure SOI [9]; but at the centre of the squares, the ⟨1 3 0⟩ directionality no longer exists. At higher Ge coverages (>4 ML), the square patterns disappear; the ⟨1 3 0⟩ directionality and the long-range order of nanocrystals are completely lost.

The third major difference is the lack of anisotropy in the shape of the nanocrystals that exists in the dewetting of pure Si. SEM and AFM imaging of nanocrystal shapes confirms that there are no facets on islands near the initiation points of the agglomeration. Figure 3(*a*) shows a

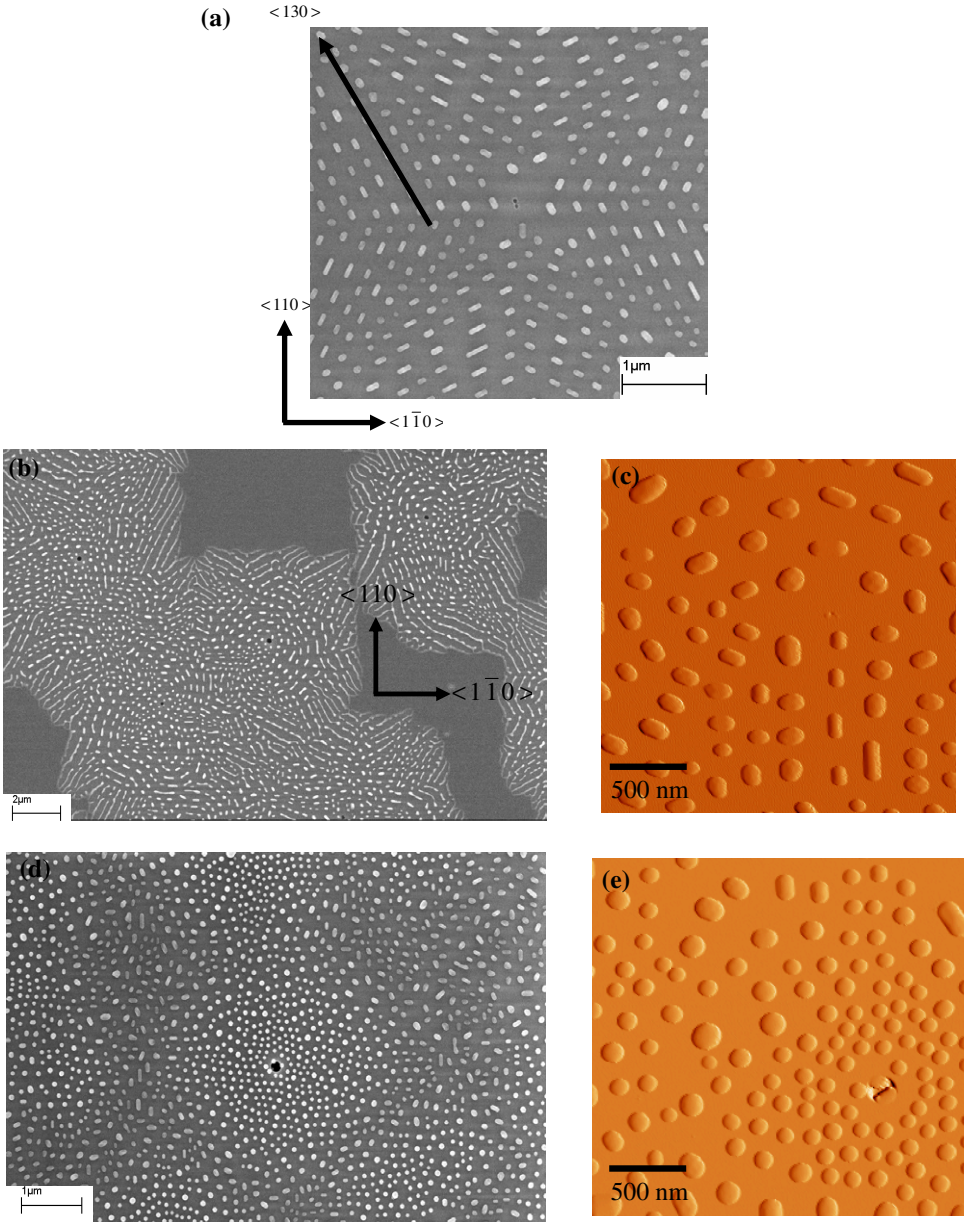

Figure 2. Thermal dewetting and agglomeration of a 9 nm layer of Si(0 0 1) in SOI, with different amounts of Ge deposited with MBE at 510 °C. (*a*) SEM image for 0 ML Ge coverage, annealed at 900 °C for 5 min. Islands are self-aligned along the ⟨1 3 0⟩ directions. (*b*) Higher-resolution SEM image than figure 1 for 2 ML Ge coverage, annealed at 850 °C for 20 s. (*c*) AFM image of the centre of an agglomerated region for 2 ML Ge coverage. Islands close to the dewetting initiation site are still faceted but do not display any long-range ordering. (*d*) Higher-resolution SEM image than figure 1 for 6 ML Ge coverage, annealed at 850 °C for 20 s. (*e*) AFM image of a central region in 6 ML Ge covered agglomerated area. Islands are not faceted, and the ⟨1 3 0⟩ directionality and long-range order of islands are completely lost.

grazing-takeoff-angle SEM image of an agglomerated 4 ML Ge/9 nm SOI surface. The agglomerated islands around the initiation sites for dewetting are rounded throughout and without facets. Under these conditions, the nanocrystals appear cylindrical with spherical caps, and are ∼100 nm in diameter and approximately the same height. The lack of facets is also proved by the AFM image in figure 3(*b*). Figure 3(*c*) shows an AFM image of an island far away from a defect. The island is still facetted, but not predominantly bounded by the {3 1 1} facets.

Dewetting of thin, thermodynamically unstable layers from a substrate (e.g., Si from SOI) and subsequent agglomeration into 3D nanostructures is driven by a desire to minimize free energy. Real-time low-energy electron microscopy (LEEM) measurements of the thermal dewetting of pure Si(0 0 1) from the oxide in SOI(0 0 1) were explained in terms of a selective surface faceting mechanism that governs the thermal agglomeration [9]. The agglomeration proceeds with sequential formation of Si trenches, ridges, and islands. Controlled by a highly selective surface faceting process, surface structures at the different stages are all predominantly bounded by {3 1 1} facets. Consequently, trenches, ridges, and hence 3D Si islands will only form along the ⟨1 3 0⟩ directions, i.e., along the intersection line of the (3 1 1) and (0 0 1) planes

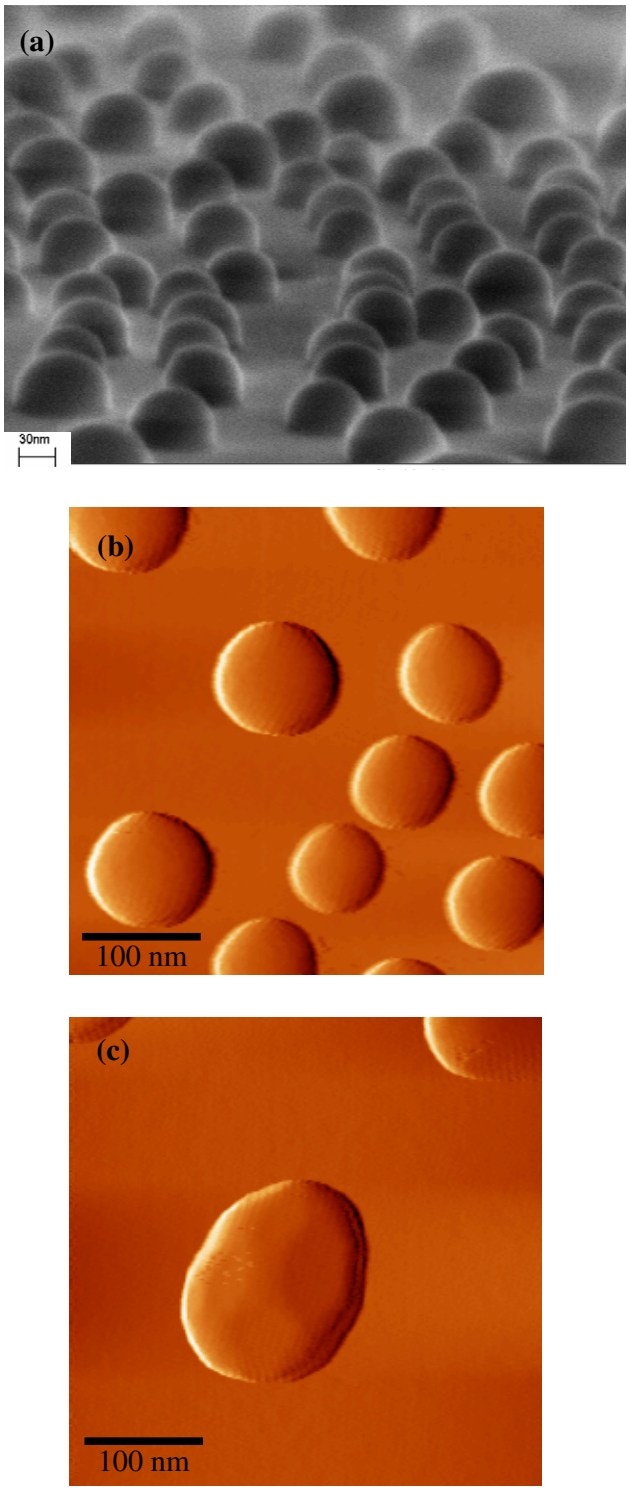

Figure 3. Thermal dewetting and agglomeration of 4 ML Ge/9 nm Si in SOI after heating for 20 s at 850 °C. (*a*) Grazing-takeoff-angle SEM image of the agglomeration region near a dewetting initiation site. (*b*) AFM image of the agglomeration region near a dewetting initiation site. SiGe islands are rounded in shape without any facets. (*c*) AFM image of one 3D island far away from the defect. The island is bounded by facets, but they are not predominantly {3 1 1}.

calculated as $(3\,\bar{1}\,1) \otimes (0\,0\,1) = \langle 1\,3\,0\rangle$. For SOI with Ge adsorbed, the formation of agglomerated 3D islands involves an energy balance between the sum of surface energies of these 3D islands and SiO_2 on the one hand and the Si–SiO_2 interface energy on the other. It should be noted that Si and Ge are miscible and that as Si dewets it alloys with the Ge. The overall formation energy of a 3D Si(Ge) agglomerated island can be calculated as

$$E_{\text{formation}} = \gamma_{\text{f}} \cos\theta + 1/2(\gamma_{\text{i}} - \gamma_{\text{Si(Ge)}} - \gamma_{\text{SiO}_2}),$$

where f, i, Si(Ge), and SiO_2 refer, respectively, to the surface energies of a facet, the 3D Si(Ge)–SiO_2 interface, the Si(Ge)(0 0 1) surface and the SiO_2 surface. For pure Si, facets exist on the 3D islands and an explanation of the observed facets in terms of the thermodynamics can be made [9]. The major difference is that Ge modifies the values of γ_{i} and $\gamma_{\text{Si(Ge)}}$ (and therefore γ_{f}). Adding Ge to Si causes both a chemical change (weaker Ge–Ge and Ge–Si bonds compared with Si–Si bonds) and creates strain. The value of $\gamma_{\text{S(iGe)}} = \gamma_{\text{bonds}} + \gamma_{\text{strain}}$ is less anisotropic than that for Si because of both of these terms. Weaker bonds make the differences between different facets smaller and strain globally reduces the stability of the film. The net result is a Wulff plot with much reduced or absent cusps at the orientations at which facets exist for Si islands. The interface energy γ_{i} is affected for the same reason.

The observed thermal agglomeration phenomenon correlates well with the Ge-induced lowering of surface roughening temperature [13], where introduction of Ge monolayers reduces chemical bonding in the system. The greater the Ge coverage, the lower the roughening temperature is [13]. As the surface roughens, its surface free energy also becomes more isotropic. Based on the observations that at fixed nominal Ge coverage (e.g. 2 ML) the agglomerated SiGe islands become less facetted and lose directional ordering for the ones closer to an initiation site, we can deduce that, for fixed nominal coverage, the islands near the initiation sites for dewetting have a higher Ge concentration than those far away from these sites. This observation implies that diffusional kinetics is also involved in the dewetting process. The introduction of Ge on Si(0 0 1) enhances surface diffusion [18, 19], via weaker bonding and increased strain.

To confirm the non-uniform Ge concentration distribution, we have performed surface sensitive scanning AES studies of the relative local Ge surface concentrations on a thermally agglomerated 6 ML Ge/SOI surface. Figure 4(*a*) shows an SEM image of the agglomerated sample. We select two different regions, one close to the initiation site and the other away from it, as indicated by small rectangles in figure 4(*a*). Figure 4(*b*), showing the Ge $L_3M_{45}M_{45}$ Auger line, confirms what we have inferred from figure 2, namely that the Ge surface concentration is non-uniform and much higher at the dewetting initiation sites.

For Ge deposition on Si(0 0 1) at 510 °C, pyramids with {1 0 5} facets, so-called huts, form on the surface when the Ge coverage is beyond three monolayers [20]. At high growth temperatures, islands of two distinctive shapes coexist on the surface, the huts and multifaceted domes [21]. Dewetting of the thin crystalline Si layer of SOI in the presence of Ge can be initiated at defects in the thin Si film, or directly around the Ge dome 'nanostressors' [22], depending on the amount of Ge heteroepitaxially grown on the surface. At the low Ge

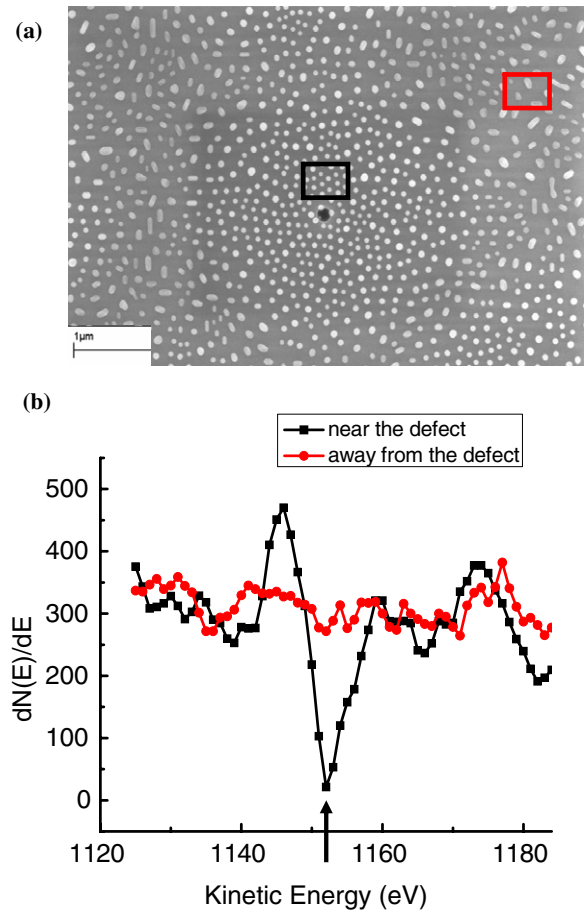

Figure 4. AES analysis of the Si and Ge concentrations in the agglomeration regions close to and away from a dewetting initiation site. (*a*) SEM image of a thermally agglomerated 6 ML Ge/9 nm Si in SOI sample heated at 850 °C for 20 s. The black square indicates a region close to the initiation site. The red square indicates a region away from the site. (*b*) AES analysis of Ge concentration in these two regions. The Ge LMM Auger line is clearly observed in the region close to the initiation site, but very weakly away from the site; demonstrating that Ge is concentrated around the dewetting initiation sites.

coverages we investigate, the dewetting starts from the intrinsic defects in the ultrathin SOI (as is the case for pure Si dewetting [9]), including HF defects, crystal-orientated particles (COPs), dislocations, stacking faults and oxide precipitates [10] or at deliberately created edges (via patterning). These defect sites generally have a lower chemical potential and behave as sinks for adatoms [23]. When Ge adatoms are deposited on SOI, the chemical-potential difference will cause preferred nucleation of domes at these sites and thus a concentration gradient around these sites (so-called denuded zone). Ge in these regions will continue to diffuse towards these defects and nucleate there, resulting in a non-uniform Ge distribution on the surface, independent of the nucleation of 'hut' islands, which can occur in parallel. This event occurs more easily during the high-temperature annealing. The formation of hut islands does not disturb this picture because huts rapidly limit their size (the growth mechanism is entirely different) and thus do not act as continuous sinks. Although we also expect Si adatom diffusion on the surface because of Ge/Si exchange [24], Ge diffuses much faster than Si, especially on a compressively strained surface [18, 19].

The increased local Ge concentration and preferred 3D dome island formation around defects create a second path for the agglomeration process in a manner that is not possible for pure Si. It has been observed that Si surrounding large Ge domes will diffuse into them, leading to the formation of a trench around the domes [25–28]. This erosion of the Si substrate, which occurs on both bulk Si substrates [25–27] and on SOI substrates [28], is caused partly by the non-uniform stress distribution around the Ge domes, in particular the large compressive stress at the dome edge [27]. One therefore has two drivers for agglomeration: a free edge or defect, and a trench created by a Ge-rich dome. When the domes are formed near dewetting initiation sites such as edges (which are the favoured sites because the chemical potential is lower there), the dome-induced Si substrate erosion adds to the drive to agglomerate.

To test the above proposal, we deposit 1.6 nm Ge on pre-patterned 20 nm SOI at 700 °C in the MBE system. We deliberately deposit Ge to this high coverage and at this high temperature to form dome clusters away from edges and pinholes. The pattern in the Si template layer is composed of mesas with variable sizes from 5 to 20 μm. Areas between the mesas have been etched down to the bottom Si handle wafer. As mentioned earlier, in addition to pinholes and other defects reaching the oxide, patterned edges are initiators of the thermal dewetting and agglomeration. For pure Si, at this temperature, no dewetting and agglomeration would be noticeable [29]. Figure 5(*a*) shows an SEM image of a sample on which 1.6 nm of Ge had been deposited at 700 °C. Clearly, the Si template layer near the pattern edges has already begun to agglomerate. Ge accumulating at the edges (diffusing there because of the chemical-potential gradient) will initiate the agglomeration at a lower temperature than will occur for pure Si. An AFM image of a section of the mesa like that in figure 5(*b*) along the direction perpendicular to the edge illustrates that the domes have eaten down to the buried oxide layer and caused agglomeration. In areas away from a patterned edge, 20 nm thick SOI will not dewet and agglomerate at 700 °C, for the 5 and 10 μm mesas as demonstrated in figure 5(*a*), because no domes have nucleated (the diffusion distance is large enough for Ge to reach the preferential edge sites). If we increase the mesa size to 20 μm, the diffusion distance is now no longer large enough and dewetting and agglomeration will occur on the mesa, because Ge domes can build up at the centre of the mesas and get large enough to create trenches in the Si. The zoom-in image of such an area, figure 5(*c*), makes this point clearly. In comparison with the isolated domes at which no dewetting has yet occurred, in the dewetted/agglomerated regions, once the process has started it continues to extend its reach. This experiment supports our conclusions in two ways. First, Ge is indeed non-uniformly distributed on the surface, with a higher concentration at the defects, and it enhances the local thermal dewetting and agglomeration of the Si template layer. Second, large enough Ge 3D islands, the so-called domes, via a strain-driven desire for alloying with the underlying Si, etch the latter to create another channel for initiation of dewetting.

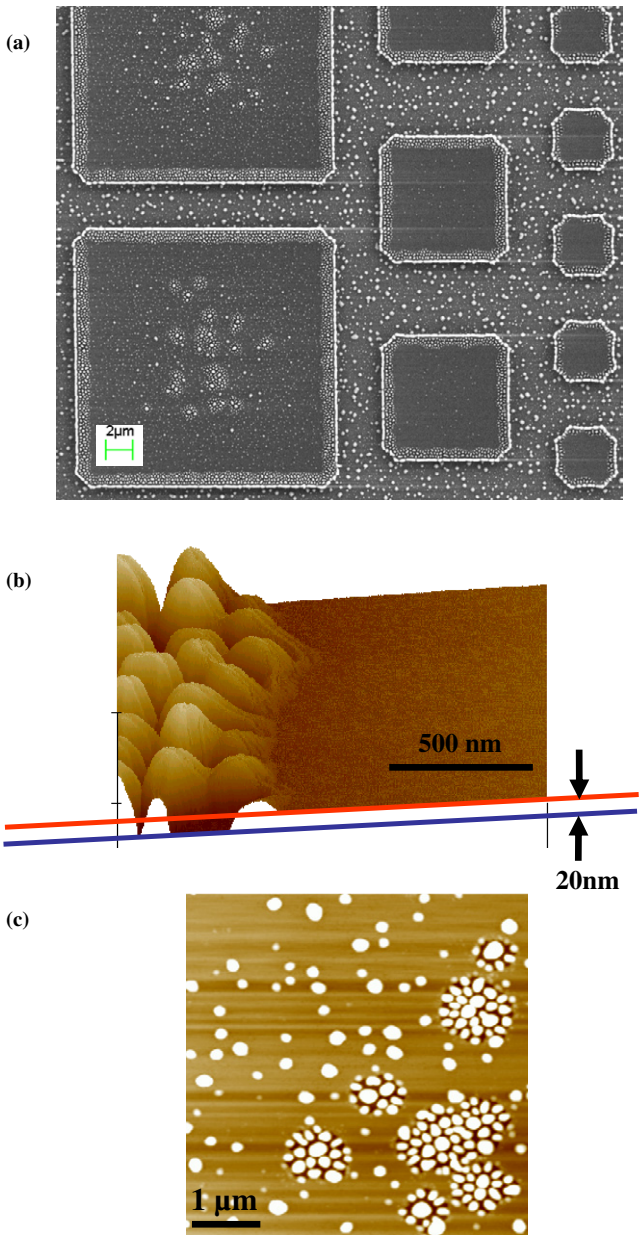

Figure 5. (*a*) SEM image of a nominal 1.6 nm Ge film deposited on patterned 20 nm SOI at 700 °C with MBE. The mesas are 5 μm, 10 μm, and 20 μm wide respectively, from right to left in the image. The large Ge domes next to the edges and the largest Ge domes randomly distributed in the centre of the widest mesas trigger the Si film to dewet and agglomerate. Agglomerated 3D islands are clearly shown in the AFM scan along the direction perpendicular to the pattern edge (*b*) and also in the magnified image of the centre of a 20 μm mesa where dewetting has begun (*c*).

4. Conclusions

In summary, we have investigated the effects of the addition of Ge on the thermal dewetting and agglomeration of the ultrathin Si template layer in SOI(0 0 1). We observe that Ge lowers the onset temperature for dewetting and agglomeration of ultrathin SOI(0 0 1) to as low as 700 °C and removes the long-range ordering of 3D islands. The lowering of the dewetting/agglomeration temperature can be explained by the weakening of chemical bonds and by the misfit strain induced by the introduction of Ge, which correlates well with the Ge-induced lowering of surface roughening temperature [13]. The lower dewetting/agglomeration temperature may restrict processing temperatures for ultrathin SGOI or for ultrathin SOI on which Ge is grown.

Acknowledgments

This research was supported by DOE Grant #DE-FG02-03ER46028 and #DE-FG02-03ER46027, NSF/MRSEC Grant #DMR0520527, and AFOSR Grant #FA9550-06-1-0487.

References

[1] Asaro R J and Tiller W A 1972 *Metall. Trans.* **3** 1789
Grinfeld M A 1993 *J. Nonlinear Sci.* **3** 35
[2] Srolovitz D J and Goldiner M G 1995 *JOM* **47** 31
[3] Hummel R E, Dehoff R T, Mattsgoho S and Goho W M 1981 *Thin Solid Films* **78** 1
[4] Jiran E and Thompson C V 1990 *J. Electron. Mater.* **19** 1153
[5] Kenneflick C M and Raj R 1989 *Acta. Metall. Mater.* **37** 2947
[6] Nuryadi R, Ishikawa Y and Tabe M 2000 *Appl. Surf. Sci.* **159** 121
[7] Legrand B, Agache V, Nys J P, Senez V and Stievenard D 2000 *Appl. Phys. Lett.* **76** 3271
[8] Nuryadi R, Ishikawa Y, Ono Y and Tabe M 2002 *J. Vac. Sci. Technol.* B **20** 167
[9] Yang B, Zhang P P, Savage D E, Lagally M G, Lu G H, Huang M H and Liu F 2005 *Phys. Rev.* B **72** 235413
[10] Danielson D T, Sparacin D K, Michel J and Kimerling L C 2006 *J. Appl. Phys.* **100** 083507
[11] Dornel E, Barbe J C, de Crecy F and Lacolle G 2006 *Phys. Rev.* B **73** 115427
[12] Yang B *et al* 2005 *Appl. Phys. Lett.* **86** 263107
[13] Maxson J B, Savage D E, Liu F, Tromp R M, Reuter M C and Lagally M G 2000 *Phys. Rev. Lett.* **85** 2152
[14] Tezuka T, Sugiyama N, Mizuno T and Takagi S 2003 *IEEE. Trans. Electron Devices* **50** 1328
[15] Yeo Y C, Subramanian V, Kedzierski J, King T J, Bokor J, Hu C M and Xuan P Q 2000 *IEEE. Electron Device Lett.* **21** 161
[16] Cheng Z Y, Currie M T, Leitz C M, Taraschi G, Fitzgerald E A, Hoyt J L and Antoniadas D A 2001 *IEEE. Electron Device Lett.* **22** 321
[17] Meuris M, Mertens P W, Opdebeeck A, Schmidt H F, Depas M, Vereecke G, Heyns M M and Philipossian A 1995 *Solid State Technol.* **38** 109
[18] Huang L, Liu F and Gong X G 2004 *Phys. Rev.* B **70** 155320
[19] Huang L, Liu F, Lu G H and Gong X G 2006 *Phys. Rev. Lett.* **96** 016103
[20] Mo Y W, Savage D E, Swartzentruber B S and Lagally M G 1990 *Phys. Rev. Lett.* **65** 1020
[21] Ross F M, Tromp R M and Reuter M C 1999 *Science* **286** 1931
[22] Sutter E and Sutter P 2006 *Nanotechnology* **17** 3724
[23] Yang B, Liu F and Lagally M G 2004 *Phys. Rev. Lett.* **92** 025502
[24] Lu Z Y, Liu F, Wang C Z, Qin X R, Swartzentruber B S, Lagally M G and Ho K M 2000 *Phys. Rev. Lett.* **85** 5603
[25] Chaparro S A, Zhang Y and Drucker J 2000 *Appl. Phys. Lett.* **76** 3534
[26] Seifert W, Carlsson N, Johansson J, Pistol M E and Samuelson L 1997 *J. Cryst. Growth.* **170** 39
[27] Spencer B J and Tersoff J 2001 *Phys. Rev.* B **63** 205424
[28] Mateeva E, Sutter P and Lagally M G 1999 *Appl. Phys. Lett.* **74** 567
[29] Ishikawa Y, Kumezawa M, Nuryadi R and Tabe M 2002 *Appl. Surf. Sci.* **190** 11